ARTICLE
Journal of Cellular Biochemistry 107:58–64 (2009)

Journal of Cellular Biochemistry

Synergy Between anti-CCL2 and Docetaxel as Determined by DW-MRI in a Metastatic Bone Cancer Model

Stefan Rozel,[1] Craig J. Galbán,[2] Klaas Nicolay,[1] Kuei C. Lee,[2] Sudha Sud,[3] Chris Neeley,[3] Linda A. Snyder,[4] Thomas L. Chenevert,[2] Alnawaz Rehemtulla,[2] Brian D. Ross,[2] and Kenneth J. Pienta[3*]

[1]*Biomedical NMR, Department of Biomedical Engineering, Eindhoven, University of Technology, Eindhoven, The Netherlands*

[2]*Departments of Radiology and Radiation Oncology, Center for Molecular Imaging, University of Michigan, Ann Arbor, Michigan 48109-2200*

[3]*Departments of Internal Medicine and Urology, University of Michigan Comprehensive Cancer Center, Michigan Center for Translational Pathology, Ann Arbor, Michigan 48109*

[4]*Ortho Biotech Oncology Research and Development, Centocor, 145 King of Prussia Road, Radnor, Pennsylvania 19087*

ABSTRACT

Metastatic prostate cancer continues to be the second leading cause of cancer death in American men with an estimated 28,660 deaths in 2008. Recently, monocyte chemoattractant protein-1 (MCP-1, CCL2) has been identified as an important factor in the regulation of prostate metastasis. CCL2, shown to attract macrophages to the tumor site, has a direct promotional effect on tumor cell proliferation, migration, and survival. Previous studies have shown that anti-CCL2 antibodies given in combination with docetaxel were able to induce tumor regression in a pre-clinical prostate cancer model. A limitation for evaluating new treatments for metastatic prostate cancer to bone is the inability of imaging to objectively assess response to treatment. Diffusion-weighted MRI (DW-MRI) assesses response to anticancer therapies by quantifying the random (i.e., Brownian) motion of water molecules within the tumor mass, thus identifying cells undergoing apoptosis. We sought to measure the treatment response of prostate cancer in an osseous site to docetaxel, an anti-CCL2 agent, and combination treatments using DW-MRI. Measurements of tumor apparent diffusion coefficient (ADC) values were accomplished over time during a 14-day treatment period and compared to response as measured by bioluminescence imaging and survival studies. The diffusion data provided early predictive evidence of the most effective therapy, with survival data results correlating with the DW-MRI findings. DW-MRI is under active investigation in the pre-clinical and clinical settings to provide a sensitive and quantifiable means for early assessment of cancer treatment outcome. J. Cell. Biochem. 107: 58–64, 2009.

KEY WORDS: PROSTATE CANCER; CHEMOTHERAPY; MACROPHAGES

It is projected by the American Cancer Society that in 2008, 186,320 men will develop prostate cancer within the United States [Jemal et al., 2008]. Prostate cancer is the second most common form of cancer in American men with an estimated 28,660 deaths in 2008, which makes it the second most common cause of cancer death. Although primary hormone deprivation therapy is successful in most men, many patients develop hormone refractory prostate cancer. Hormone refractory prostate cancer is non-curative and has a high incidence of metastatic disease, with ~90% of patients with advanced prostate cancer developing bone lesions [Bubendorf et al., 2000].

Recently, several reports have indicated that chemokines have an important role in the regulation of tumorigenesis, contributing to cancer progression of several adenocarcinomas including breast and prostate cancer [Youngs et al., 1997; Vanderkerken et al., 2002]. CCL2 is a member of the chemokine family that has been shown to

Grant sponsor: NIH; Grant number: PO1 CA093900; Grant sponsor: American Cancer Society Clinical Research Professorship; Grant sponsor: NIH SPORE in Prostate Cancer Grant; Grant number: P50 CA69568; Grant sponsor: Cancer Center Support Grant; Grant number: P30 CA46592; Grant sponsor: SouthWest Oncology Group; Grant number: CA32102; Grant sponsor: Prostate Cancer Foundation.

*Correspondence to: Kenneth J. Pienta, MD, 7308 CCC, 1500 E. Medical Center Drive, Ann Arbor, MI 48109-5946. E-mail: kpienta@umich.edu

Received 15 December 2008; Accepted 16 December 2008 • DOI 10.1002/jcb.22056 • 2009 Wiley-Liss, Inc.
Published online 3 March 2009 in Wiley InterScience (www.interscience.wiley.com).

attract monocytes and macrophages to the tumor site inducing an inflammatory response which promotes tumor growth. This macrophage invasion is shown to be the predominant mechanism by which CCL2 stimulates tumor growth [Loberg et al., 2007a]. In addition, CCL2 has been shown to have a direct promotional effect on tumor cell proliferation, migration, and survival [Loberg et al., 2007a]. Previous studies have shown that mouse (C1142) and human (CNTO888) CCL2 antibodies (anti-CCL2) given in combination with docetaxel were able to induce tumor regression in a pre-clinical prostate cancer model [Loberg et al., 2007b].

A limitation in the drug development process for evaluating new treatments for metastatic prostate cancer is the inability of imaging to objectively assess response to treatment. Current imaging strategies to evaluate early treatment response in metastatic prostate cancer residing within bone in the clinic are unavailable [Hamaoka et al., 2004], and the Response Evaluation Criteria in Solid Tumors (RECIST) system explicitly mentions bone tumors to be non-measurable [Therasse et al., 2000]. This emphasizes the importance of developing and implementing new imaging methods for measurement of treatment response for this disease. Diffusion-weighted MRI (DW-MRI) holds great promise for assessing response to anticancer therapies. DW-MRI can be used to quantify the random (i.e., Brownian) motion of water molecules within intact living tissue [Moffat et al., 2004]. This imaging approach is very appealing as a biomarker of early treatment response as the diffusion of water molecules within a tumor are hindered by cellular membranes. Successful treatment, which results in the loss of tumor cells, reduces the barriers which impede the mobility of the water molecules. DW-MRI provides an imaging method for quantification of water diffusion values and is reported as an apparent diffusion coefficient (ADC). ADC values will increase in tumor regions experiencing a loss of cellular density. This principle was first demonstrated using a chemotherapy-treated rodent glioma model [Ross et al., 1994] and was subsequently validated in a variety of pre-clinical studies assessing the response to anticancer agents including cytotoxic and cytostatic therapies, radiation therapy, and gene therapy [Zhao et al., 1996; Chenevert et al., 1997, 2000, 2002; Hakumaki et al., 1998; Poptani et al., 1998; Ross et al., 1998, 2003; Galons et al., 1999; Chinnaiyan et al., 2000; Stegman et al., 2000; Jennings et al., 2002; Hall et al., 2004; Hamstra et al., 2004; Moffat et al., 2004; Theilmann et al., 2004; Jordan et al., 2005; Schepkin et al., 2006; Lee et al., 2006a,b, 2007a,b,c; Kim et al., 2008]. Treatment-induced changes in tumor ADC values were found to occur early and prior to tumor volumetric changes providing the rationale for using this imaging biomarker as an early predictive marker of treatment response [Chenevert et al., 2000]. Thus, DW-MRI is under active investigation in the pre-clinical and clinical settings to provide a sensitive and quantifiable means for early assessment of cancer treatment outcome.

We have recently reported that DW-MRI can provide an early indication of treatment response in tumors located within the skeletal system using a mouse model of metastatic prostate cancer to the bone [Lee et al., 2007c]. Furthermore, we have also demonstrated the feasibility of using DW-MRI in a patient with metastatic hormone sensitive prostate cancer which demonstrated a correlation between diffusion changes and a decrease in PSA levels consistent with a positive treatment response [Lee et al., 2007d]. The current study is aimed at measuring the treatment response of prostate cancer in an osseous site to docetaxel, an anti-CCL2 agent, and combination treatments using DW-MRI to evaluate if this imaging biomarker can differentiate between different therapeutic interventions.

MATERIALS AND METHODS

CELL LINES

The PC3 human androgen independent cancer cell line is derived from a human prostate cancer metastasis to bone. The PC3 cells were transfected with a luciferase-expressing plazarus retroviral construct as previously described [Kalikin et al., 2003]. Luciferase produces light in the presence of Luciferin and oxygen, making the transfected cells distinguishable from the host rodent cells using a bioluminescence imaging system (BLI). Wild-type PC3 cells were cultured in RPMI 1640 supplemented with 10% fetal bovine serum, while transfected $PC3^{luc}$ were maintained in selection media supplemented with 200 μg/ml G418.

AGENTS

Anti-CCL2 antibodies, C1142 and CNTO888 were supplied by Centocor, Inc., CNTO888 is a human $IgG_1\kappa$ antibody that neutralizes human CCL2. C1142 is a rat/mouse chimeric antibody that neutralizes mouse CCL2. Anti-CCL2 therapy consisted of simultaneous administration of both antibodies. Docetaxel (Taxotere) was obtained from the University of Michigan Hospital Pharmacy.

MICE

Male severe combined immunodeficient mice (SCID, T-cell and B-cell deficient) were purchased from Charles River (Wilmington, MA). The mice were housed in pathogen-free rooms at the University of Michigan internationally accredited facilities in microisolator cages. Mice were anesthetized using a 2% isofluorane/air mixture and 2×10^5 $PC3^{luc}$ cells were introduced by intracardiac injection in the left ventricle. $PC3^{luc}$ cells spread throughout the body and typically produced several sites of bone metastases. Two separate groups of animals were prepared for these studies. Study I consisted of a total of 48 animals which were used to evaluate the effects of the experimental treatments on tumor control. Study II consisted of a total of 40 animals from which 23 were selected to undergo MRI and BLI. Study I animals began treatments 2 weeks after cell inoculation whereas Study II animals began treatments once tumors became of sufficient size to study by MRI (~6–12 μl).

BLI

To identify mice with bone metastases in the tibia, BLI was performed 4 weeks after $PC3^{luc}$ injection using a highly sensitive CCD camera (IVIS 200; Caliper Life Sciences, Alameda, CA). All animals from Study II entered the bioluminescence study ($n = 40$), and based on the bioluminescence images a subset was selected ($n = 23$) to enter the MRI study. To perform BLI, mice were anesthetized with a 2% isofluorane/air mixture and 150 mg/kg D-luciferin was administered by intraperitoneal injection. Ten to 12 min after IP injection, bioluminescence images were acquired

using a FOV of 25 cm, a binning factor of 2, f/1 lens setting and an exposure time of 15 s. The mice were kept under anesthesia in the bioluminescence detector using a nose cone system to deliver the isofluorane/air mixture and the animal stage was heated to 37°C to maintain the core body temperature of the animal.

Previous efforts had found that bioluminescence photon counts were directly proportional to the number of tumor cells; allowing for quantification of the number of tumor cells in a lesion [Lee et al., 2007c; Loberg et al., 2007b]. A baseline bioluminescence scan was acquired before initiation of treatment. After initiation of treatment bioluminescence scans were acquired each week until the animals were euthanized. Regions of interest (ROI) were manually drawn around the animals using the Living Image™ software 2.5 provided with the BLI system. The photon count (photons/s) within an ROI was used as a quantitative measure of the total tumor burden in the animals. The photon counts collected throughout the study were normalized to the photon counts measured at baseline. This approach provided for the measurement of treatment response and disease progression over time.

TREATMENT

Study I. The effects of docetaxel, anti-CCL2 and a combination of the two agents were evaluated and compared to untreated (PBS treated) animals using bioluminescence imaging to follow the growth of $PC3^{luc}$ cells in mice ($n = 12$ mice per group). Animals began treatment two weeks following cell inoculation. Animals treated with docetaxel were dosed with 40 mg/kg/week for 3 weeks while anti-CCL2 was administered at 10 mg/kg twice weekly for the duration of the study. BLI was conducted weekly on each of the animals. Quantification of photon counts was accomplished at each time point, and an average value was determined for each group of mice over time to allow for quantification of temporal changes in "tumor burden" for the different treatment groups. Animals were euthanized when they became moribund.

Study II. Twenty-three animals were selected to enter the MRI study which were divided into four groups; an untreated group ($n = 4$), a docetaxel treated group ($n = 10$, 40 mg/kg/week for 3 weeks), an anti-CCL2 treated group ($n = 4$, 10 mg/kg twice weekly until animals became moribund) and a combination group treated with docetaxel and anti-CCL2 ($n = 5$, docetaxel 40 mg/kg/week for 3 weeks and anti-CCL2 10 mg/kg twice weekly until animals became moribund).

MRI

During MRI examinations, animals were anesthetized with 1.5% isofluorane/air mixture and their body temperatures maintained at 37°C using an Air-Therm heater (World Precision Instruments, Sarasota, FL). MRI images were acquired on a Varian 9.4 T animal MR-scanner (120 mm horizontal bore; Varian, Palo Alto, CA) using a 20 mm volume SAW coil (M2M imaging, Cleveland, OH). The animal's leg was suspended in the center of the coil by attaching to the toe a ligature which was fastened to the coil frame. T_2-weighted anatomical images were acquired using a fast spin-echo sequence with the following parameters: FOV = 20 × 20 mm; TR/TE = 4000/52 ms; echo train length = 8; echo spacing = 13 ms; 24 interleaved slices (contiguous); thickness = 0.5 mm; matrix = 256 × 128; 2 signal averages. DW images were acquired using a spin-echo sequence, with a navigator echo and gradient waveforms sensitive to isotropic diffusion [Moffat et al., 2004], with the following parameters: FOV = 20 × 20 mm; TR/TE = 4000/37 ms; 18 interleaved slices (contiguous); thickness = 0.5 mm; gap = 0.1 mm; matrix = 128 × 128 (readout × phase); averages = 1; b values = 120 s/mm^2 and 1200 s/mm^2. Placement of the slice package for the DW images was based on lesion position as determined from the anatomical images.

STATISTICAL ANALYSIS

Repeated measures analyses of variance were conducted on tumor burden assuming first-order autocorrelation covariance structures. Natural splines were used to flexibly model the curvature of trends in the time profiles. Comparisons between the groups were performed at each of the time points using a Student's t-test. Logarithmic transformations were performed prior to analyses to better satisfy the underlying statistical modeling assumptions of equal variance and sampling from populations with normal distributions. Time to disease-related death was evaluated using life table methods. The log-rank test was used for comparisons among treatment groups. *P*-values less than 0.05 were considered significant.

RESULTS

OVERALL TREATMENT RESPONSE AND SURVIVAL (STUDY I ANIMALS)

To evaluate the long-term impact of docetaxel and anti-CCL2 antibody therapy, an experiment was performed to measure the effects of treatment on prostate cancer growth in mice (Fig. 1).

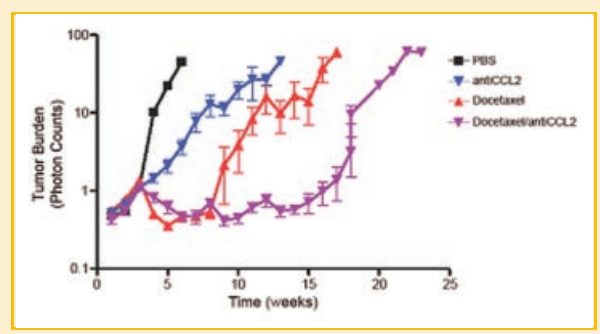

Fig. 1. Measurement of total body tumor burden over time for Study I animals bearing $PC3^{luc}$ tumor cells as quantified by BLI photon counts. Animals representing the four treatment groups are shown. Mean ± SEM is shown for each group; tumor burden is shown while 8 of 12 mice remained on study for each group. Mice were treated with docetaxel at weeks 2, 3, and 4 at 40 mg/kg; anti-CCL2 antibodies were administered at 2 mg/kg twice a week starting at week 2 and continuing for the duration of the study. All treatment groups showed significantly reduced tumor burden as compared to the PBS group from weeks 4 to 6 ($P < 0.001$); both docetaxel treatment groups showed significantly reduced tumor burden as compared to the anti-CCL2 antibody group from weeks 4–8 ($P \leq 0.013$); the docetaxel/anti-CCL2 group showed significantly reduced tumor burden as compared to docetaxel alone from weeks 9 to 12 ($P \leq 0.021$).

Animals were sacrificed per protocol when the animals became moribund or tumor burden by photon count reached maximum tolerated count [Loberg et al., 2007b]. Significant inhibition in tumor growth rates were observed by BLI for all test groups, with the combination of docetaxel and anti-CCL2 treatment having the greatest effect, followed by docetaxel and anti-CCL2, which had slightly reduced growth rates over control animals. The reduction in tumor growth rates in the treated animals was reflected in animal survival for the different treatment groups (Fig. 2). Overall survival was found to be greatest with the combination docetaxel/anti-CCL2 antibody group followed by docetaxel alone and anti-CCL2. Median survival for control animals was 6 weeks, anti-CCL2 antibodies: 11 weeks ($P = 0.006$ vs. PBS control); docetaxel alone: 15 weeks ($P = 0.021$ vs. anti-CCL2 antibodies); and combination therapy: 22 weeks ($P < 0.001$ vs. any other group). These results demonstrate that combination therapy of docetaxel/anti-CCL2 antibodies was more effective than either monotherapy to prolong tumor growth inhibition and extend survival.

EVALUATION OF IMAGING BIOMARKERS OF TREATMENT RESPONSE (STUDY II ANIMALS)

A separate group of animals (Study II) was prepared to evaluate the ability of DW-MRI to detect differential responses to the therapies based upon differences in the magnitude of changes in tumor water diffusion values. Initial BLI was done for all animals (n = 40) at 4 weeks post-intracardiac $PC3^{luc}$ injection to identify those animals with intratibial lesions. A subset of animals (n = 23) that showed metastatic disease in the tibia was selected to enter the MRI study and treatment was initiated following baseline MRI scans. Animals from the control group and the anti-CCL2 group demonstrated a continuous increase in the bioluminescence signal intensity over the first 14 days of the experiment as shown in Figure 3. Animals from the docetaxel-treated group and the group of animals treated with the combination of docetaxel and anti-CCL2 demonstrated a stable to decreasing bioluminescence signal over the 14-day period of the experiment. Since the photon counts quantified from each lesion are proportional to the number of luciferase positive PC3 cells present, it would be anticipated that the volume of the tumors would also reflect the relative changes (or lack thereof) in the BLI signal levels.

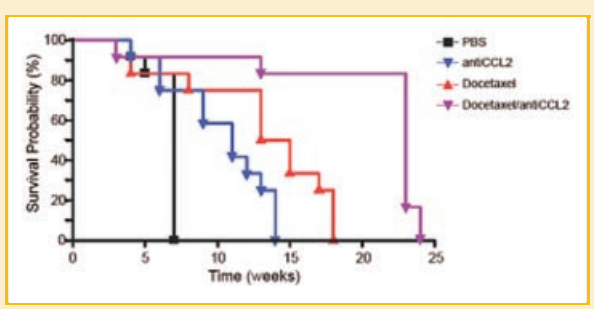

Fig. 2. Animal survival plot for $PC3^{luc}$ inoculated animals for each of the treatment groups in Study I. Mice were treated with docetaxel at weeks 2, 3, and 4 at 40 mg/kg; anti-CCL2 antibodies were administered at 2 mg/kg twice a week starting at week 2 and continuing for the duration of the study.

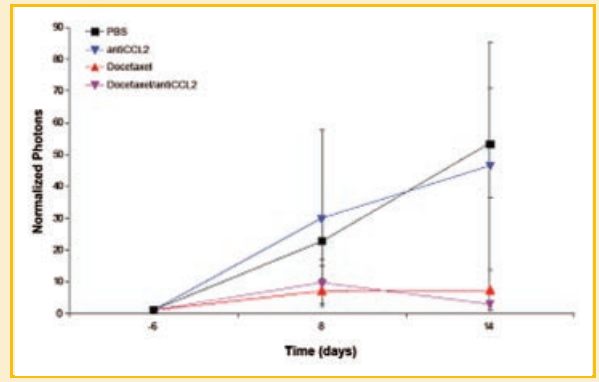

Fig. 3. Bioluminescence imaging data pre- and post-treatment initiation for Study II treated animals. Normalized photons are presented for control (black square), anti-CCL2 (blue inverted triangle), docetaxel (red triangle), and the combination of docetaxel and anti-CCL2 treated animals (purple inverted triangle) at days −6, 8 and 14 post treatment initiation. Data displayed as mean ± SEM.

In this regard, tumor volumes for individual animals were obtained over time using anatomical T_2-weighted MRI. The control and anti-CCL2 treated groups showed a continuous increase in tumor volume up to an 8.0-fold increase and 6.5-fold increase on day 14, respectively. Although not significant, the anti-CCL2 treated group had a slightly diminished growth rate relative to the untreated group. The docetaxel and combination docetaxel/anti-CCL2 treated groups demonstrated stable tumor volumes and slight regression, respectively based upon the MRI-determined volumetric measurements (Fig. 4). When comparing the docetaxel treated group or the combination group to the control group, a significant reduction in tumor volumes were found on days 6 and 10 ($P < 0.05$).

DW-MRI was also used to evaluate the treatments in the Study II animals since this imaging modality is sensitive for the detection of cell death rather than cell cycle arrest. Measurements of tumor ADC values were accomplished over time during the 14-day treatment

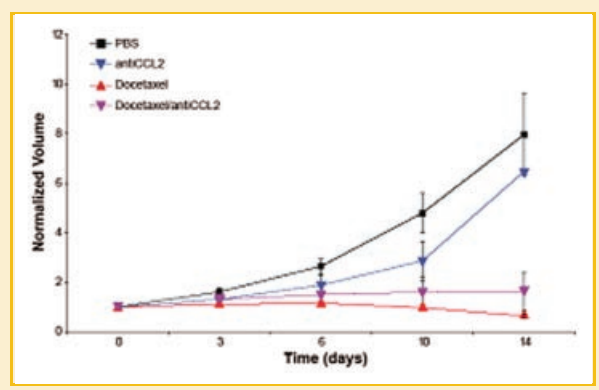

Fig. 4. Normalized tumor volumes from tibial PC3 tumors obtained over time using MRI (Study II). Values shown are from baseline (day 0) and at days 3, 6, 10, and 14 post-treatment initiation. Normalized tumor volume presented correspond to control (black square), anti-CCL2 (blue inverted triangle), docetaxel (red triangle), and the combination of docetaxel and anti-CCL2 treated animals (purple inverted triangle). Data displayed as mean ± SEM.

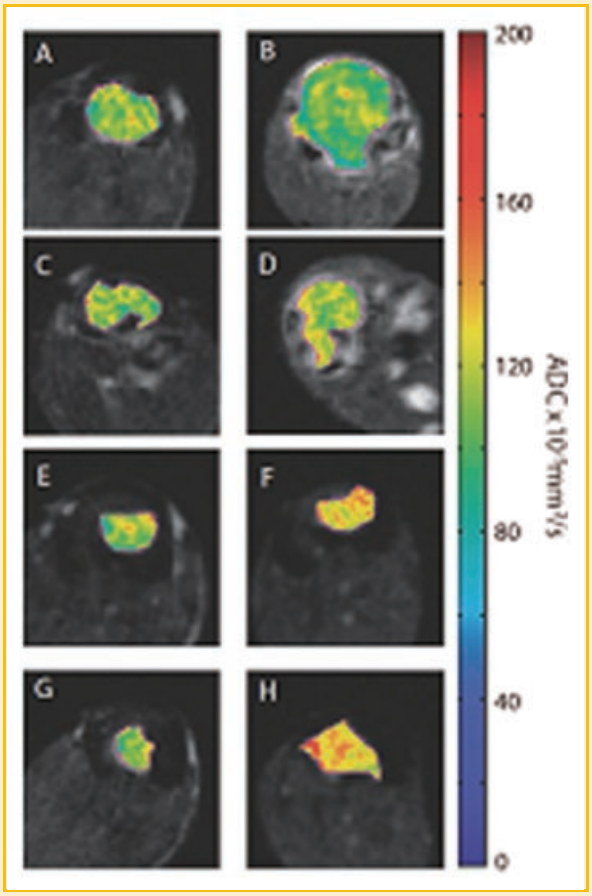

Fig. 5. Representative ADC maps of PC3 tumor shown as color overlays on T_2-weighted images (Study II). ADC maps were acquired pre-treatment (day 0) (left column) and 14 days post-treatment initiation (right column). Image pairs are from four different animals representing control (A,B), anti-CCL2 (C,D), docetaxel (E,F) and combination therapy with docetaxel and anti-CCL2 therapy (G,H). Color scale represents tumor ADC values 0 to 200 $\times$ 10^{-5} mm^2/s.

period. Shown in Figure 5 are quantitative ADC values displayed as a color overlay on the anatomical T_2-weighted MR images from representative animals from each of the four treatment groups at baseline (Fig. 5A,C,E,G) and at 14 days post-treatment initiation (Fig. 5B,D,F,H). The color overlays reveal the quantitative ADC values on a voxel-by-voxel basis for the tumors at baseline (day 0) and at 14 days post-treatment initiation. Baseline tumor diffusion values reveal relatively low diffusion of between 90 and 125 $\times$ 10^{-5} mm^2/s (yellow to green color). Small pockets of higher diffusion values are observable pre-treatment which can likely be attributable to focal areas of spontaneous necrosis within the tumor mass. Following 14 days of therapy, it is apparent that the docetaxel (Fig. 5F) and combination of docetaxel and anti-CCL2 (Fig. 5H) treated animals had the largest shift in ADC values as evidenced by the large amount of yellow to red color-encoded voxels within the tumor mass. In addition to ADC, these images provide for observing the relative changes in tumor volumes for each animal. Quantification of tumor diffusion values was accomplished at each time point from ROI's drawn to circumscribe the tumor volume. Control (PBS)

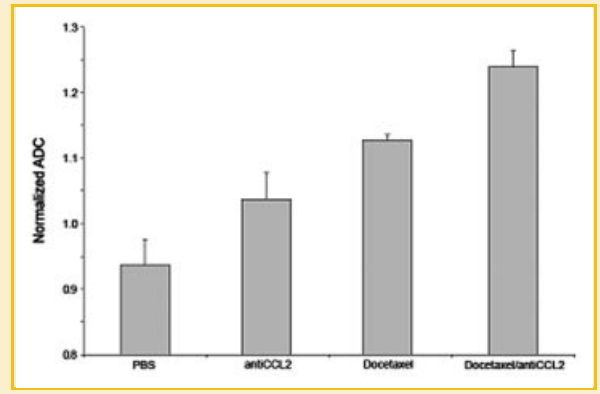

Fig. 6. PC3 tumor ADC values 14 days following therapy normalized to baseline (Study II). Data displayed as mean $\pm$ SEM.

and anti-CCL2 treatment groups generated stable mean ADC values throughout the 14-day treatment period (data not shown). As shown in Figure 6, combination of docetaxel and anti-CCL2 treatment groups had the most significant increase in ADC values ($P < 0.05$) as compared to all other groups. Significant differences were not observed between the other groups. The anti-CCL2 group, due to attrition of animals and negligible changes in ADC, was pooled over days 10 and 14.

DISCUSSION

In this current study, DW-MRI was used to evaluate differential effects of docetaxel, anti-CCL2 and a combination of docetaxel and anti-CCL2 treatments on PC3 tumor growth in a mouse bone tumor model. It was previously shown by Loberg et al. [2007b] using BLI that anti-CCL2 treatment was able to slow tumor growth rate as well as delay tumor recurrence after docetaxel treatment was stopped. Moreover, a previous study had also found that docetaxel was able to induce tumor regression and that DW-MRI was able to detect a tumor response before significant tumor volume changes were observed [Lee et al., 2007c]. Based upon these previous studies, this series of experiments was undertaken to evaluate the ability of DW-MRI to detect differences in treatment-associated changes in tumor cellularity using water diffusion as a surrogate marker in single and combination agents of docetaxel and anti-CCL2 during the early phase of treatment.

MRI-determined tumor volume data (Fig. 4) revealed that there was an attenuation of tumor growth rate between the control and anti-CCL2 treated groups (growth rate for control is 0.52 vs. 0.45 for anti-CCL2 treated with the growth rate defined as the power in the exponential fit through the volume data). The docetaxel and docetaxel + anti-CCL2 treatment groups both inhibited tumor growth similarly over the course of the 14-day imaging study. Tumor volume measurements over the 2-week period were incapable of delineating any synergy between anti-CCL2 and docetaxel from docetaxel alone. Moreover, BLI was also not able to detect differences in tumor cell kill values between the docetaxel and combination groups as both groups displayed similar stable

photon counts over time (Fig. 3). Furthermore, the control and anti-CCL2 groups produced increasing BLI photon counts over time with no differences between them. As the error bars were fairly large, additional numbers of animals may possibly allow for a more definitive conclusion.

The use of imaging to provide feedback related to the efficacy of a treatment has been a subject of great interest. In this study, we also utilized DW-MRI in an effort to see if this quantitative imaging method could detect differences in efficacy between the treatment groups. Diffusion of water molecules within the tumor mass is affected by the number of tumor cells present per unit volume, as cell membranes limit the movement of water molecules thus restricting their diffusion or Brownian motion. During treatments which result in a net loss of cellular membranes, diffusion values increase in those regions. Therefore, by quantification of the changes in tumor water diffusion values using DW-MRI during treatment, it should in principle be possible to differentiate between treatments which have different therapeutic effectiveness.

In this study, diffusion measurements of PC3 tumors over time revealed increases in water ADC values in response to both docetaxel and combined docetaxel with anti-CCL2 treatments. However, as shown in Figure 6, the combination therapy group revealed a larger increase in diffusion values at day 14 as compared with the docetaxel alone. The diffusion data provided early evidence that the more effective therapy would be anticipated to be the combination group as the combination therapy was found to have the largest overall increased change in diffusion values. Animal survival data (Fig. 2) revealed that the combination therapy, in fact, provided enhanced survival over docetaxel alone, thus corroborating the DW-MRI findings. The anti-CCL2 treatment may inhibit the attraction of macrophages to the tumor site. As previously noted, these macrophages promote a chronic inflammation which can result in stimulation of tumor growth. However, this feature was not found as there appeared to be a modest decrease in tumor growth rates and improved survival with anti-CCL2 treatment.

In conclusion, the magnitude of the changes in tumor diffusion values as quantified by DW-MRI were determined to provide an early readout of changes in tumor cellularity during the treatments administered in this study, and were reflective of overall impact on tumor growth and animal survival. Measurement of tumor ADC values and comparing these values to BLI measurements provide complementary information. However, DW-MRI can be translated in the clinical setting and as such, it is possible to use this imaging biomarker in Phase I, II, or III clinical trials.

ACKNOWLEDGMENTS

K.J. Pienta is supported by NIH grant CA093900, an American Cancer Society Clinical Research Professorship, NIH SPORE in prostate cancer grant P50 CA69568, Cancer Center support grant P30 CA 46592, NIH ICMIC P50 CA93990, NIH SAIRP U24 CA083099 and the Southwest Oncology Group CA32102, the Prostate Cancer Foundation, a Ralph Wilson Medical Research Foundation Grant, a Wallace H. Coulter Foundation Translational Partners Seed Grant as well as a contract from Centocor. BDR, AR, and TLC have a financial interest in the underlying DW-MRI technology. We thank Dr. Paul Marsters of Centocor for conducting the statistical analysis for the in vivo efficacy study.

REFERENCES

Bubendorf L, Schopfer A, Wagner U, Sauter G, Moch H, Willi N, Gasser TC, Mihatsch MJ. 2000. Metastatic patterns of prostate cancer: An autopsy study of 1,589 patients. Hum Pathol 31:578–583.

Chenevert TL, McKeever PE, Ross BD. 1997. Monitoring early response of experimental brain tumors to therapy using diffusion magnetic resonance imaging. Clin Cancer Res 3:1457–1466.

Chenevert TL, Stegman LD, Taylor JM, Robertson PL, Greenberg HS, Rehemtulla A, Ross BD. 2000. Diffusion magnetic resonance imaging: An early surrogate marker of therapeutic efficacy in brain tumors. J Natl Cancer Inst 92:2029–2036.

Chenevert TL, Meyer CR, Moffat BA, Rehemtulla A, Mukherji SK, Gebarski SS, Quint DJ, Robertson PL, Lawrence TS, Junck L, Taylor JM, Johnson TD, Dong Q, Muraszko KM, Brunberg JA, Ross BD. 2002. Diffusion MRI: A new strategy for assessment of cancer therapeutic efficacy. Mol Imaging 1:336–343.

Chinnaiyan AM, Prasad U, Shankar S, Hamstra DA, Shanaiah M, Chenevert TL, Ross BD, Rehemtulla A. 2000. Combined effect of tumor necrosis factor-related apoptosis-inducing ligand and ionizing radiation in breast cancer therapy. Proc Natl Acad Sci USA 97:1754–1759.

Galons JP, Altbach MI, Paine-Murrieta GD, Taylor CW, Gillies RJ. 1999. Early increases in breast tumor xenograft water mobility in response to paclitaxel therapy detected by non-invasive diffusion magnetic resonance imaging. Neoplasia 1:113–117.

Hakumaki JM, Poptani H, Puumalainen AM, Loimas S, Paljarvi LA, Yla-Herttuala S, Kauppinen RA. 1998. Quantitative 1H nuclear magnetic resonance diffusion spectroscopy of BT4C rat glioma during thymidine kinase-mediated gene therapy in vivo: Identification of apoptotic response. Cancer Res 58:3791–3799.

Hall DE, Moffat BA, Stojanovska J, Johnson TD, Li Z, Hamstra DA, Rehemtulla A, Chenevert TL, Carter J, Pietronigro D, Ross BD. 2004. Therapeutic efficacy of DTI-015 using diffusion magnetic resonance imaging as an early surrogate marker. Clin Cancer Res 10:7852–7859.

Hamaoka T, Madewell JE, Podoloff DA, Hortobagyi GN, Ueno NT. 2004. Bone imaging in metastatic breast cancer. J Clin Oncol 22:2942–2953.

Hamstra DA, Lee KC, Tychewicz JM, Schepkin VD, Moffat BA, Chen M, Dornfeld KJ, Lawrence TS, Chenevert TL, Ross BD, Gelovani JT, Rehemtulla A. 2004. The use of 19F spectroscopy and diffusion-weighted MRI to evaluate differences in gene-dependent enzyme prodrug therapies. Mol Ther 10:916–928.

Jemal A, Siegel R, Ward E, Hao Y, Xu J, Murray T, Thun MJ. 2008. Cancer statistics, 2008. CA Cancer J Clin 58:71–96.

Jennings D, Hatton BN, Guo J, Galons JP, Trouard TP, Raghunand N, Marshall J, Gillies RJ. 2002. Early response of prostate carcinoma xenografts to docetaxel chemotherapy monitored with diffusion MRI. Neoplasia 4:255–262.

Jordan BF, Runquist M, Raghunand N, Baker A, Williams R, Kirkpatrick L, Powis G, Gillies RJ. 2005. Dynamic contrast-enhanced and diffusion MRI show rapid and dramatic changes in tumor microenvironment in response to inhibition of HIF-1alpha using PX-478. Neoplasia 7:475–485.

Kalikin LM, Schneider A, Thakur MA, Fridman Y, Griffin LB, Dunn RL, Rosol TJ, Shah RB, Rehemtulla A, McCauley LK, Pienta KJ. 2003. In vivo visualization of metastatic prostate cancer and quantitation of disease progression in immunocompromised mice. Cancer Biol Ther 2:656–660.

Kim H, Morgan DE, Buchsbaum DJ, Zeng H, Grizzle WE, Warram JM, Stockard CR, McNally LR, Long JW, Sellers JC, Forero A, Zinn KR. 2008. Early therapy evaluation of combined anti-death receptor 5 antibody and

gemcitabine in orthotopic pancreatic tumor xenografts by diffusion-weighted magnetic resonance imaging. Cancer Res 68:8369–8376.

Lee KC, Hall DE, Hoff BA, Moffat BA, Sharma S, Chenevert TL, Meyer CR, Leopold WR, Johnson TD, Mazurchuk RV, Rehemtulla A, Ross BD. 2006a. Dynamic imaging of emerging resistance during cancer therapy. Cancer Res 66:4687–4692.

Lee KC, Hamstra DA, Bullarayasamudram S, Bhojani MS, Moffat BA, Dornfeld KJ, Ross BD, Rehemtulla A. 2006b. Fusion of the HSV-1 tegument protein vp22 to cytosine deaminase confers enhanced bystander effect and increased therapeutic benefit. Gene Ther 13:127–137.

Lee KC, Hamstra DA, Bhojani MS, Khan AP, Ross BD, Rehemtulla A. 2007a. Noninvasive molecular imaging sheds light on the synergy between 5-fluorouracil and TRAIL/Apo2L for cancer therapy. Clin Cancer Res 13: 1839–1846.

Lee KC, Moffat BA, Schott AF, Layman R, Ellingworth S, Juliar R, Khan AP, Helvie M, Meyer CR, Chenevert TL, Rehemtulla A, Ross BD. 2007b. Prospective early response imaging biomarker for neoadjuvant breast cancer chemotherapy. Clin Cancer Res 13:443–450.

Lee KC, Sud S, Meyer CR, Moffat BA, Chenevert TL, Rehemtulla A, Pienta KJ, Ross BD. 2007c. An imaging biomarker of early treatment response in prostate cancer that has metastasized to the bone. Cancer Res 67:3524–3528.

Lee KC, Bradley DA, Hussain M, Meyer CR, Chenevert TL, Jacobson JA, Johnson TD, Galban CJ, Rehemtulla A, Pienta KJ, Ross BD. 2007d. A feasibility study evaluating the functional diffusion map as a predictive imaging biomarker for detection of treatment response in a patient with metastatic prostate cancer to the bone. Neoplasia 9:1003–1011.

Loberg RD, Ying C, Craig M, Yan L, Snyder LA, Pienta KJ. 2007a. CCL2 as an important mediator of prostate cancer growth in vivo through the regulation of macrophage infiltration. Neoplasia 9:556–562.

Loberg RD, Ying C, Craig M, Day LL, Sargent E, Neeley C, Wojno K, Snyder LA, Yan L, Pienta KJ. 2007b. Targeting CCL2 with systemic delivery of neutralizing antibodies induces prostate cancer tumor regression in vivo. Cancer Res 67:9417–9424.

Moffat BA, Hall DE, Stojanovska J, McConville PJ, Moody JB, Chenevert TL, Rehemtulla A, Ross BD. 2004. Diffusion imaging for evaluation of tumor therapies in preclinical animal models. MAGMA 17:249–259.

Poptani H, Puumalainen AM, Grohn OH, Loimas S, Kainulainen R, Yla-Herttuala S, Kauppinen RA. 1998. Monitoring thymidine kinase and ganciclovir-induced changes in rat malignant glioma in vivo by nuclear magnetic resonance imaging. Cancer Gene Ther 5:101–109.

Ross BDCT, Kim B, Ben-Yoseph O. 1994. Magnetic resonance imaging and spectroscopy: Application to experimental neuro-oncology. Quart Magn Reson Biol Med 1:89–106.

Ross BD, Zhao YJ, Neal ER, Stegman LD, Ercolani M, Ben-Yoseph O, Chenevert TL. 1998. Contributions of cell kill and posttreatment tumor growth rates to the repopulation of intracerebral 9L tumors after chemotherapy: An MRI study. Proc Natl Acad Sci USA 95:7012–7017.

Ross BD, Moffat BA, Lawrence TS, Mukherji SK, Gebarski SS, Quint DJ, Johnson TD, Junck L, Robertson PL, Muraszko KM, Dong Q, Meyer CR, Bland PH, McConville P, Geng H, Rehemtulla A, Chenevert TL. 2003. Evaluation of cancer therapy using diffusion magnetic resonance imaging. Mol Cancer Ther 2:581–587.

Schepkin VD, Lee KC, Kuszpit K, Muthuswami M, Johnson TD, Chenevert TL, Rehemtulla A, Ross BD. 2006. Proton and sodium MRI assessment of emerging tumor chemotherapeutic resistance. NMR Biomed 19:1035–1042.

Stegman LD, Rehemtulla A, Hamstra DA, Rice DJ, Jonas SJ, Stout KL, Chenevert TL, Ross BD. 2000. Diffusion MRI detects early events in the response of a glioma model to the yeast cytosine deaminase gene therapy strategy. Gene Ther 7:1005–1010.

Theilmann RJ, Borders R, Trouard TP, Xia G, Outwater E, Ranger-Moore J, Gillies RJ, Stopeck A. 2004. Changes in water mobility measured by diffusion MRI predict response of metastatic breast cancer to chemotherapy. Neoplasia 6:831–837.

Therasse PAS, Eisenhauer EA, Wanders J, Kaplan RS, Rubinstein L, Verweij J, VanGlabbeke M, VanOosterom AT, Christian MC, Gwyther SG. 2000. New guidelines to evaluate the response to treatments in solid tumors. J Natl Cancer Inst 92:205–216.

Vanderkerken K, Vande Broek I, Eizirik DL, Van Valckenborgh E, Asosingh K, Van Riet I, Van Camp B. 2002. Monocyte chemoattractant protein-1 (MCP-1), secreted by bone marrow endothelial cells, induces chemoattraction of 5T multiple myeloma cells. Clin Exp Metastasis 19:87–90.

Youngs SJ, Ali SA, Taub DD, Rees RC. 1997. Chemokines induce migrational responses in human breast carcinoma cell lines. Int J Cancer 71:257–266.

Zhao M, Pipe JG, Bonnett J, Evelhoch JL. 1996. Early detection of treatment response by diffusion-weighted 1H-NMR spectroscopy in a murine tumour in vivo. Br J Cancer 73:61–64.